Published in final edited form as:
Microcirculation. 2011 April ; 18(3): 228–237. doi:10.1111/j.1549-8719.2011.00082.x.

Matrix Metalloproteinase Activity Causes VEGFR-2 Cleavage and Microvascular Rarefaction in Rat Mesentery

Edward D. Tran[1], **Ming Yang**[2], **Andrew Chen**[1], **Frank A. DeLano**[1], **Walter L. Murfee**[2], and **Geert W. Schmid-Schönbein**[1]

[1] Department of Bioengineering, The Whitaker Institute for Biomedical Engineering University of California San Diego La Jolla, CA 92093-0412

[2] Department of Biomedical Engineering Tulane University New Orleans, LA 70118

Abstract

A complication of the spontaneously hypertensive rat (SHR) is microvascular rarefaction, defined by the loss of microvessels. However, the molecular mechanisms involved in this process remain incompletely identified. Recent work in our laboratory suggests that matrix metalloproteinases (MMPs) may play a role by cleavage of the vascular endothelial growth factor receptor 2 (VEGFR-2). In order to further delineate the role for MMPs in microvascular rarefaction, the objective of the current study was to examine the relationship in the same tissue between MMP activity, VEGFR-2 cleavage and rarefaction. Using an *in-vivo* microzymographic technique we show significantly enhanced levels of MMP-1, -1/-9, -7, and -8 activities, but not MMP-2 and-3 activities, along mesenteric microvessels of the SHR compared to its normotensive control, Wistar Kyoto (WKY) rat. Based on immunohistochemical methods, the SHR exhibited a decreased labeling of the extracellular, but not the intracellular, domain of VEGFR-2 along mesenteric microvessels. Chronic MMP inhibition served to attenuate VEGFR-2 cleavage and microvascular network rarefaction in the SHR mesentery. These results spatially link MMP-induced VEGFR-2 cleavage and rarefaction in the mesentery of the SHR and thus support the hypothesis that MMPs serve as regulators of microvascular dysfunction in hypertension.

Keywords

Spontaneously Hypertensive Rat; Wister Kyoto rat; capillary; arteriole; venule; microzymography; matrix metalloproteinase inhibition

INTRODUCTION

A common characteristic of genetic hypertension is microvascular rarefaction, defined by a loss of microvessels, including small arterioles, venules, and/or capillaries (5,8,16,18,22). While rarefaction has been associated with endothelial apoptosis (7,20), increased oxidative stress, and inflammation, the causal molecular mechanisms remain to be identified (11,21).

Recently, we identified a role for matrix metalloproteinase (MMP) activity in hypertension associated microvascular dysfunction (4,19). MMPs cause cleavage of the extracellular domain of insulin receptor leading to insulin resistance. In the spontaneously hypertensive

Correspondence: Dr. Geert W. Schmid-Schönbein Department of Bioengineering, The Whitaker Institute for Biomedical Engineering University of California San Diego La Jolla, CA 92093-0412 Tel: 858 534-3852 Fax: 858 534-5722 gwss@bioeng.ucsd.edu .

rat (SHR) chronic inhibition of MMPs with a broad acting inhibitor, doxycycline, has been shown to prevent this receptor cleavage, normalize blood pressure and decrease oxygen free radical production (4). Chronic MMP inhibition also attenuated vascular endothelial growth factor receptor 2 (VEGFR-2) cleavage (19). Relevant to microvascular rarefaction, VEGFR-2 signaling is critical for endothelial cell viability (15) and its depletion leads to capillary regression (1,6,13). Our previous work served to identify a causal relationship between elevated plasma levels of MMP activity with VEGFR-2 cleavage along microvessels in cardiac tissues and vessel loss in the cremaster muscle (19). In order to establish a local role for MMPs in microvascular rarefaction, the objective of the current study was to examine the relationship in the same tissue between MMP activity, VEGFR-2 cleavage and rarefaction.

Accordingly we used a microzymographic technique to determine *in-vivo* the activity levels of selected MMPs in the mesenteric microcirculation of the SHR, and its normotensive Wistar Kyoto control (WKY) strain. Fluorogenic substrates specific for MMP-1, -1/-9, -2, -3, -7, and -8, were utilized, and their cleavage into fluorescent products was measured in all classes of rat mesenteric microvessels. The selection of these specific MMPs was based on previous work form our laboratory (4,19) identifying elevated MMP-2, MMP -1/-9 and MMP-7 activity in SHR compared to the activity in WKY plasma. We determined the level of VEGFR-2 proteolytic cleavage in the mesentery and its association with capillary rarefaction after chronic MMP inhibition. We used doxycycline, a member of the tetracycline family, which is an FDA-approved MMP inhibitor and usable in future clinical studies. This work serves to add to our understanding of the role of MMP activity in microvascular rarefaction within a tissue that has been well associated with hypertension induced vessel specific dysfunction.

MATERIALS AND METHODS

Fluorogenic Substrates

The following *fluorogenic substrates* were purchased (from American Peptide Company, APC, Sunnyvale, CA; and Sigma-Aldrich, St. Louis, MO):

Vascular Collagenase: MMP-1 (collagenase, or murine collagenase-like A and B in the rat), Dnp-Pro-Cha-Abu-Cys(Me)-His-Ala-Lys(N-Me-Abz)-NH2, 1.5 μM, excitation at 365 nm and emission at 450 nm, APC; and MMP-8 (Neutrophil Collagenase) Dnp-Pro-Leu-Ala-Tyr-Trp-Ala-Arg, 1.5 μM, ex/em 280/360 nm, APC.

Gelatinase: MMP-2 (Gelatinase A), Mca-Pro-Leu-Ala-Nva-Dpa-Ala-Arg-NH2, 1.5 μM, ex/em 350/385 nm, Sigma; and MMP-1/-9 (for Collagenase and Gelatinase B), N-(2,4-Dinitrophenyl)-Pro-Leu-Gly-Leu-Trp-Ala-D-Arg, 1.5 μM ex/em 280/346 nm, Sigma.

Stromelysin: MMP-3 (Stromelysin-1), MOCAc-Arg-Pro-Lys-Pro-Tyr-Ala-Nva-Trp-Met-Lys-(DNP)-NH2, 1.5 μM, ex/em 325/395 nm, Sigma.

Matrilysin: MMP-7 (Matrilysin-1), Dnp-Arg-Pro-Leu-Ala-Leu-Trp-Arg-Ser, 1.5 μM, ex/em 278/358 nm, APC.

The specificity of the fluorogenic substrates was validated with their purified enzyme MMPs (Calbiochem, Gibbstown, NJ). The fluorogenic MMP substrates were incubated with the different purified MMPs, 37°C 30 min in dark. The fluorescence level of each well was recorded with a fluorescent microscope. The fluorogenic MMP substrates and their respective (specific) MMPs have significantly higher fluorescence level comparing to the substrates alone (auto-fluorescence) or with other (non-specific) MMPs. Pro-MMPs were

activated with 2-aminophenylmercuric acetate (APMA). To block MMP activity, we used the broad-spectrum MMP inhibitors doxycycline (West-Ward Pharmaceutical Corp., Eatontown, N.J.), GM6001 (Calbiochem), and the iron chelator ethylenediaminetetraacetic acid (EDTA, Fisher Scientific).

Animals

All experimental protocols were reviewed and approved by the University of California San Diego Animal Subjects Committee. After general anesthesia (sodium Nembutal, 50 mg/kg body weight, Abbott Laboratories, North Chicago, IL, USA, i.m.), male SHRs and normotensive WKY rats (Charles River Laboratories, Wilmington, MA, USA; 12-18 weeks, 280-350 g) were placed on a water-heated stage (37°C) and cannulated with a femoral artery and vein catheter (PE50, I.D. 0.5 mm/ O.D. 0.956 mm, Becton Dickinson Primary Care Diagnostics, Sparks, MD). Mean arterial pressure and heart rate were digitally recorded (MacLab with Macintosh G3). Supplemental doses of anesthesia (5 mg/kg) were administered intravenously as indicated after reflex testing. At the end of the study, the animals were euthanized (pentobarbital 120 mg/kg body weight, i.v.).

Subgroups of the SHRs and WKY rats were treated with the broad blocking MMP inhibitor, doxycycline (55 mg/liter in drinking water, ~ 5.4 mg/kg/day) as previously described (4). The number of rats in each group was six.

Mesentery Preparation

The abdominal cavity was exposed via a mid-line incision. The intestinal mesentery was loosely draped over an observation window by carefully manipulating the intestine with cotton-tipped applicators. To avoid drying and hyperosmotic injury, the exposed intestine and adjacent mesenteric sections were covered with sponge gauze and kept continuously superfused with Krebs-Henseleit solution (pH 7.4, 305 mOsm, 37°C).

Microvascular Observations

The mesenteric microcirculation was viewed with 10× and 40× water-immersion lens (Zeiss, Oberkochen, Germany) on an intravital microscope (Leica Microsystems GmbH, Wetzlar, Germany) at a resolution sufficient to observe longer segments of microvessels and detect non-uniformities of enzyme activity. Bright-field and fluorescent images were recorded with a color charge-coupled device camera (Model VI-470, Optronics, Goleta, CA) and stored with a DVD recorder (Sony DVO 1000MD). Selected tissue areas were recorded for the full duration of the experiment. Bright-field intravital microscopy was used to detect microvessel morphology; fluorescent microscopy was used to detect substrate cleavage.

The exteriorized mesentery was superfused with Krebs-Henseleit solution and MMP substrates. Bright-field and simultaneous fluorescent images of selected mesenteric capillaries and their surrounding tissue parenchyma were recorded. The exposure time to fluorescent light was kept below 10 seconds per image with one image per 15-minute interval for a total observation period of one hour. Pilot experiments showed that this low exposure frequency caused no detectable apoptosis (detected by propidium iodide labeling) due to the light *per se* (20).

Digital In-vivo Microzymography

Protease activity in the microcirculation was determined from the fluorescent signal of the intramolecularly-quenched fluorescent substrates after cleavage by enzymes. Similar to previously described methods (4), each mesentery was loaded with a single substrate (for concentrations see list of Reagents above) 10 minutes prior to image collection and continuously suffused with substrate throughout the experiment. The associated

fluorescence was visualized by fluorescent intravital microscopy and recorded digitally (Fig. 1). Measurements reported in this study were made at 60 min from the time of the continuous superfusion.

Measurements of fluorescent intensity were obtained along microvessels (average light intensity units over a length of 100 μm). Multiple measurements were grouped by tissue region, per vessel category (arterioles, capillaries, and venules). Means were computed for all regions of a single mesentery sector of an animal and then averaged for all animals in each group. For each tissue section suffused with a substrate, the enzymatic activity of the enzyme is correlated with the fluorescent product precipitated on the tissue through a cleavage process. The density of the fluorescent product can be estimated by measuring the light emission, E, of the tissue section, defined as, $E = \log_{10} (I_{60}/I_0)$, where I_{60} represents the average light intensity value along the vessel at 60 minutes after the substrate was loaded and I_0 represents the auto-fluorescence measured immediately after the substrate was loaded.

VEGFR-2 Receptor Labeling

To examine the receptor density of VEGFR-2, fresh SHR and WKY mesenteric sectors, consisting of thin translucent connective tissues connected to the small intestine and outside of adipose tissue, were collected, fixed (paraformaldehyde 4%, 1 hr, 4°C) and labeled with either a primary antibody against the extracellular or against the intracellular domain of VEGFR-2, followed by biotin/avidin labeling with horseradish peroxidase and Vector Red substrate. According to the manufacturer (Santa Cruz Biotechnology, Inc.) the binding sites for the antibodies are as follows: Flk-1 (Q-20): sc-19530 and Flk-1 (S-20): sc-48161 bind to a 20-amino acid epitope between amino acid sites 50 and 100 and a 20-amino acid epitope between amino acid sites 1,300 and 1,350, respectively. The specificity of the intracellular VEGFR-2 antibody was confirmed by an enhanced immunolabel density of cultured HUVECS that were permeabalized with saponin versus cells that were not permeabalized (Supplemental Figure 1). Positive immunolabeling in mesenteric tissues was confirmed by comparison of the labeling density without the primary antibody (Supplemental Figure 2).

Values of receptor density were obtained by light intensity measurements, analogous to the techniques described under *Digital in-vivo Micro-zymography*. In a tissue section labeled colormetrically, the density of the targeted antigen is correlated with the density of pigment precipitated on the tissue through a chromogenic process. The density of pigment can be estimated by measuring the light absorption, A, of the tissue section, defined as, $A = \log_{10} (I_0/I_{vessel})$, where I_{vessel} represents the average light intensity value along a vessel and I_0 represents the average light intensity value for a slide not containing a tissue. Doxycycline-treated SHR and WKY mesenteries were labeled with the antibody against the extracellular domain of VEGFR-2, and analyzed in a similar method.

Mesentery Microvessel Labeling and Network Analysis

Vascularized sectors of mesentery with entire microvascular networks were harvested from each of the four experimental animal groups: SHR (n = 4 animals, 6 tissues), SHR treated with Doxycycline (n = 5 animals, 9 tissues), WKY (n = 3 animals, 5 tissues), and WKY rats with Doxycycline treatment (n = 5 animals, 9 tissues). The tissues were fixed in paraformaldehyde (4%, 1 hr, 4°C) and labeled with a biotinylated monoclonal antibody against PECAM (CD31) (diluted in antibody buffer of 0.1% Saponin in PBS + 2% BSA+5% horse serum; BD Pharmingen) followed by a streptavidin-peroxidase secondary antibody (VECTASTAIN Elite ABC; Vector Laboratories) with Vector Nova Red (Vector Laboratories) substrate (14).

Images were captured using an inverted microscope (Olympus IX70) coupled with a CCD camera and a Cooke 5× dry objective (numerical aperture = 0.15). Network montages, generated by overlaying sequential images using custom software, were used to trace individual vessels and generate skeletonized networks for vascular density and area analysis. Isolated microvascular networks were identified as having at least one feeding/draining arterial/venous vessel pair. The mesentery tissue area occupied by a microvascular network was determined as the shaded area shown in Figure 2. For vessel counts per vessel category, arterioles, venules and capillaries were identified based on anatomical position within the network relative to the draining/feeding vessels and vessel morphology. Vessels less than 8 μm in diameter were considered to be capillaries and the capillary count did not include blind ended sprouts. The total number of networks per group included in the analysis was as follows: SHR (n = 17 networks), SHR with doxycycline treatment (n = 18 networks), WKY (n = 12 networks), WKY with doxycycline treatment (n = 23 networks).

Statistics

All measurements are presented as mean ± standard error. Statistical analysis of the microzymographic and VEGFR-2 immunohistochemical data was carried out by a *t* test. Statistical analysis of VEGFR-2 immunohistochemical data between WKY and SHR groups with and without doxycycline treatment was carried out by ANOVA followed by *a Student-Newman-Keuls* test for pair wise comparisons. For analysis of microvascular network architecture metrics, a Mann-Whitney Rank Sum Test was used to identify whether a difference exists between 2 specific non-normally distributed data sets per comparison independent of other groups. A t-test or Mann-Whitney Rank Sum Test was used to directly assess whether a difference exists between 2 specific data sets per comparison independent of other groups. $p < 0.05$ was considered significant.

RESULTS

MMP Activities in Mesentery Microcirculation

The fluorogenic peptide substrates gave a comprehensive picture of enzyme activity in all segments of the microcirculation of freshly exposed mesentery. At 60 minutes post the start of continuous substrate superfusion, significantly increased levels of substrate cleavage for MMP-1 MMP-1/-9, MMP-7, and MMP-8 were recorded along SHR versus WKY venules (Fig. 3). No significant increase of MMP-2 and -3 activities (data not shown) were recorded along any of the SHR microvessel segments in this preparation.

There was no significant increase of the MMP substrate intensity in the interstitium or by tissue mast cells of the mesentery for any of the substrates tested in this study. Mast cells were identified by their enlarged, round morphology and the presence of granules. Increased MMP-1, -1/-9, -7, and -8 activities in the SHR were predominantly detected along venules (versus the corresponding WKY venules at 60 min exposure; $p<0.05$ in each case) with lower activities along arterioles and capillaries (Fig. 3A). The increase of the enzyme activity in venules of the SHR was not associated with enhanced levels of leukocyte attachment to the endothelium detected by bright field intravital microscopic observation. This magnification was selected for this study in order to observe entire microvascular segments and still detect differences in enzyme activity. Previous measurements of MMP-9 activity based on immunolabeling and microzymography methods (4) indicate that endothelial cells have a heterogeneous labeling pattern so that cells with increased labeling are located side by side to cells with low labeling levels.

All MMP activities could be blocked to levels below detection limit by superfusion of the tissue with EDTA (10 mM) or GM6001 (1 μM) (4). The MMP activities were also blocked by chronic treatment of the SHR with doxycycline, as shown previously (4).

Expression of VEGFR-2

The degree of extracellular domain cleavage of VEGFR-2 was determined by use of separate antibodies against its intracellular and extracellular domain in all classes of microvessels of the SHR and WKY mesentery. The SHR had a significantly lower labeling density of the extracellular domain of VEGFR-2 along mesenteric arterioles and capillaries, and with a similar trend along mesenteric venules (not significant) (Fig. 4). The reduced label density for the extracellular domain of VEGFR-2 was observed along arterioles and capillaries in-spite of the lack of differences in MMP activity along SHR versus WKY vessels for these vessel types. No significant differences were observed for intracellular labeling between SHR and WKY vessel types.

Chronic MMP Inhibition Attenuates VEGFR-2 Cleavage in the SHR

Chronic doxycycline treatment served to attenuate the level of receptor cleavage of VEGFR-2 in mesentery. Both doxycycline-treated groups had significantly higher levels of the extracellular domain expression compared to their respective control groups (Fig. 5).

Chronic MMP Inhibition Attenuates Rarefaction in the SHR

The mesenteric tissue in the SHR exhibited typical rarefaction in form of smaller networks compared to the WKY rats (Fig. 6). Microvascular area per network (illustrated in Fig. 2) of SHR was small (1.80 ± 1.01 mm^2) compared to the control WKY group (7.58 ±3.48 mm^2; $p = 0.0039$). Similarly, microvascular length per network for the SHR group was decreased (18.63 ± 8.46 mm) compared to the control WKY group (86.74 ±36.90 mm; $p = 0.025$). Evidence for microvascular rarefaction in the SHR is also displayed by a reduction in the number of vessels per network in each category (arterioles: SHR = 12.94 ±6.36, WKY = 45.83 ±20.42, $p = 0.019$; venules: SHR = 20.06 ±9.03, WKY = 77.17 ±42.67, $p = 0.033$; capillaries: SHR = 24.18 ±9.28, WKY = 195.42 ±112.35, $p = 0.006$) (Fig. 8). After chronic doxycycline treatment vascular area (4.97 ± 1.55 mm^2; $p = 0.014$) and vascular length per network were increased (40.45 ±11.29 mm; $p = 0.025$) in the SHR group (Fig. 7). The average SHR network size and vascular length post treatment were not significantly different compared to the WKY groups (Fig. 7B). In the doxycycline treated SHR group compared to the untreated SHR group, the number of capillaries per network was increased (48.17 ±10.42; $p = 0.011$), an effect not seen for arterioles and venules and for any vessel type across the WKY groups.

Arterial Blood Pressure

The mean femoral blood pressures in the WKY rats and SHRs were 134 ± 10 and 174 ± 6 mmHg, respectively ($p < 0.05$), and these values were significantly reduced to 96 ± 8 and 126 ± 14 mmHg, respectively ($p < 0.05$), after treatment with chronic MMP blockade (doxycycline) (4).

DISCUSSION

The current results indicate that the SHR, compared to its normotensive WKY strain, has elevated MMP-1, -1/-9, -7, and -8 activity along venules in adult rat mesenteric microvascular networks. Because we minimized the time between anesthesia and exposure of the tissue and measurements of enzyme activity (< 1 hr), there was insufficient time for *de novo* synthesis of proteases suggesting that the enhanced activity is already present in the

SHR tissue before tissue exposure. Our previous studies indicate that MMP-1, -2, -1/-9 , -7, and -8 have also elevated activity in plasma collected from the femoral vein (4,19), and thus with the exception of MMP-2, are the same enzymes that exhibit enhanced activity along mesentery microvessels in the SHR. This enhanced MMP activity within mesenteric microvascular networks was associated with vessel specific VEGFR-2 cleavage and microvascular rarefaction. The attenuation of both VEGFR-2 cleavage and rarefaction by chronic systemic MMP inhibition supports the hypothesis for an involvement of MMPs in hypertension associated microvascular dysfunction. MMP activity in SHR plasma was detected by use of specific fluorescently quenched substrates and gelatin zymography (4,19). In the current study, we focused on identifying the relationship between increased MMP activity, apparent VEGFR-2 cleavage, and microvascular rarefaction in the same tissue characterized by hypertension-associated microvascular dysfunction.

The current results suggest that VEGFR-2 cleavage and microvascular rarefaction occur in the rat mesenteric tissue. MMP activity, as detected by microzymography with cleavage of fluorescently quenched MMP substrates, was observed along venules, vessels which exhibit little elevation of blood pressure in the SHR (26). The increased protease activity as detected by fluorescently quenched substrates along venules does not completely correlate with the decreased VEGFR-2 labeling along arterioles and capillaries. There may be several reasons. The fluorescent images for the current analysis of the MMP activity were collected 60 minutes after substrate superfusion over the mesentery tissue. Previous data from our laboratory (4) has shown increased MMP-1-/9 activity along SHR versus WKY arterioles, capillaries, and venules using a similar in-vivo microzymography method and measurements from images recorded10 minutes after substrate superfusion. The comparison of the current and previous analyses suggests that substrate spreading as well as fluorescent quenching may occur during the superfusion period, yielding lower fluorescent intensities especially in arterioles and capillaries, which have lower protease activity compared to venules. Additional analysis is necessary to determine the activity levels for MMP-1, -7, and along SHR versus WKY arterioles and capillaries. The possibility exists that enhanced activity along these vessel types is sufficient to cleave VEGFR2 in the SHR.

In addition to the MMP activity recorded along microvessel walls, the enhanced MMP-2, MMP-9 and MMP-7 activity in the plasma of the SHR (19) may play also a role in receptor cleavage in the mesentery microcirculation. The plasma of the SHR has the ability to cleave membrane receptors on naïve donor cells in free suspension (4). Direct application of purified MMP-7 and -9 (200 nmol/L, 6 hrs, 37°C) leads to a significant reduction of the label density of VEGFR-2 on endothelial cells (19).

Doxycycline was used in this study because 1) it does broadly inhibit MMP activity and therefore serves to identify a potential role for MMPs in hypertension related microvascular alterations; 2) doxycycline has been shown to block MMP activity in the SHR (19); and 3) to match similar MMP blocking studies (4,17,19) revealing a role of MMPs in cleavage of the extracellular domain of the insulin receptor, the VEGFR-2 and the β_2 adrenergic receptor in the SHR. Doxycycline has also been demonstrated to inhibit production of multiple MMPs by endothelial cells in culture at the mRNA level (10) suggesting that doxycycline does have a direct effect on MMP production on vascular cells. Though doxycycline is an antibiotic, our results indicating its influence on MMP activity in the rat mesentery suggests a relationship between increased blood pressure, increased MMP activity, apparent VEGFR-2 cleavage, and altered microvascular network structure. Further studies are required to identify the mechanism related to doxycline's effect and to determine to what degree doxycycline is influencing the regulation of other mechanisms potentially linked to blood pressure in the SHR. Additionally, future studies with more selective MMP blockers are required to explore the role of specific MMPs, although under the conditions of chronic

hypertension the activity of any MMP blocker needs to be nuanced since MMPs are important for many tissue repair functions.

Our previous results suggest a relationship between elevated plasma levels of MMP activity with VEGFR-2 cleavage along microvessels and endothelial cell apoptosis in rat heart (19). Chronic MMP inhibition by doxycycline was shown to attenuate the loss of capillaries in the cremaster muscle. The current results suggest that cleavage of VEGFR-2 by MMPs occurs in the same mesenteric tissue, which in the SHR is associated with microvascular rarefaction, dysfunction and endothelial apoptosis. Cleavage of the extracellular domain reduces the ability of the cell to bind VEGF agonists and may be one of the reasons for the enhanced apoptosis in the SHR endothelium (9,12,23,25). The functional effect of attenuated VEGFR-2 signaling on vessel loss is supported by observation of reduced VEGFR-2 protein levels being associated with impaired angiogenesis in the SHR (24). Our results indicate that microvascular rarefaction in the SHR compared to the WKY mesentery is detectable by a decrease in vascular area, vessel length per network and a reduction in the number of arterioles, venules, and capillaries per network (Fig. 6-8). Chronic inhibition of MMPs results in a reversal of rarefaction in SHR mesenteric networks in form of an increase in network size, vascular length, and number of capillaries. We would expect that attenuation of MMP-induced VEGFR-2 cleavage would lead to the observed increase in number of vessels. While this was the case for capillaries, this was not the case for arterioles. In our analysis, vessels with a diameter less than 8 μm were considered to be capillaries. Thus, the results might not account for any increase in the number of small pre-capillary arterioles or post-capillary venules that fall under this threshold. Whether these structural alterations are directly caused by MMP inhibition, VEGFR-2 cleavage or via a mechanism that involves the reduction of arterial blood pressure caused by MMP inhibition remains unclear.

Cleavage of the extracellular domain of VEGFR-2 in the SHR appears to be not unique to this receptor. Evidence for an increased MMP activity and receptor cleavage is also detectable by acutely exposing naïve cells or cardiac tissue of normotensive Wistar rats to SHR plasma (2,4,19,22). Based on these study designs, we have obtained evidence for cleavage of the extracellular domain of the insulin receptor α and the leukocyte adhesion receptor CD18 (4). The receptor cleavage compromises the ability of insulin to stimulate glucose transport and leukocyte adhesion, i.e. they cause Type II diabetes and immune suppression encountered in the SHR. Chronic treatment of the SHR with an MMP inhibitor restores normal cell function and attenuates this pathophysiological condition (4). Thus, the current evidence supports the hypothesis that typical cellular defects in the SHR may in fact be due to enzymatic cleavage of receptors responsible for specific cell functions.

Supplementary Material

Refer to Web version on PubMed Central for supplementary material.

Acknowledgments

This work was supported was supported by NHLBI grant HL 10881, a gift from Leading Ventures and the Tulane Hypertension and Renal Center of Excellence funded by NIH grant P20RR017659-08.

REFERENCES

1. Baffert F, Le T, Sennino B, Thurston G, Kuo CJ, Hu-Lowe D, McDonald DM. Cellular changes in normal blood capillaries undergoing regression after inhibition of VEGF signaling. Am J Physiol Heart Circ Physiol. 2006; 290:H547–59. [PubMed: 16172161]

2. Chen AY, DeLano FA, Valdez SR, Shin HY, Schmid-Schönbein GW. Receptor cleavage reduces the fluid shear response in neutrophils of the spontaneously hypertensive rat. American Journal of Physiology - Cell Physiology. 2010; 299:C1441–C1449. [PubMed: 20861466]
3. Delano FA, Parks DA, Ruedi JM, Babior BM, Schmid-Schönbein GW. Microvascular display of xanthine oxidase and NADPH oxidase in the spontaneously hypertensive rat. Microcirculation. 2006; 13:551–566. [PubMed: 16990214]
4. DeLano FA, Schmid-Schönbein GW. Proteinase activity and receptor cleavage: Mechanism for insulin resistance in spontaneously hypertensive rat. Hypertension. 2008; 52:415–423. [PubMed: 18606910]
5. Funk R, Rohen JW. Comparative morphological studies on blood vessels in eyes of normotensive and spontaneously hypertensive rats. Exp Eye Res. 1985; 40:191–203. [PubMed: 3979460]
6. Gerber HP, Hillan KJ, Ryan AM, Kowalski J, Keller GA, Rangell L, Wright BD, Radtke F, Aguet M, Ferrara N. VEGF is required for growth and survival in neonatal mice. Development. 1999; 126:1149–59. [PubMed: 10021335]
7. Gobé G, Browning J, Howard T, Hogg N, Winterford C, Cross R. Apoptosis occurs in endothelial cells during hypertension-induced microvascular rarefaction. J Struct Biol. 1997; 118:63–72. [PubMed: 9087915]
8. Hutchins PM, Darnell AE. Observations of a decreased number of small arterioles in spontaneously hypertensive rats. Circ. Res. 1974; 34-35:161–165.
9. Jiang F, Zhang X, Kalkanis SN, Zhang Z, Yang H, Katakowski M, Hong X, Zheng X, Zhu Z, Chopp M. Combination therapy with antiangiogenic treatment and photodynamic therapy for the nude mouse bearing U87 glioblastoma. Photochem Photobiol. 2008; 84:128–37. [PubMed: 18173712]
10. Hanemaaijer R, Visser H, Koolwijk P, Sorsa T, Salo T, Golub LM, van Hinsbergh VW. Inhibition of MMP synthesis by doxycycline and chemically modified tetracyclines (CMTs) in human endothelial cells. Adv Dent Res. 1998; 12(2):114–8. [PubMed: 9972133]
11. Kobayashi N, DeLano FA, Schmid-Schönbein GW. Oxidative stress promotes endothelial cell apoptosis and loss of microvessels in the spontaneously hypertensive rats. Arterioscler Thromb Vasc Biol. 2005; 25:2114–21. [PubMed: 16037565]
12. Lim HH, DeLano FA, Schmid-Schönbein GW. Life and death cell labeling in the microcirculation of the spontaneously hypertensive rat. J Vasc Res. 2001; 38:228–36. [PubMed: 11399895]
13. Meeson AP, Argilla M, Ko K, Witte L, Lang RA. VEGF deprivation-induced apoptosis is a component of programmed capillary regression. Development. 1999; 126:1407–15. [PubMed: 10068634]
14. Murfee WL, Schmid-Schönbein GW. Structure of microvascular networks in genetic hypertension. Chapter 12. Methods Enzymol. 2008; 444:271–84. [PubMed: 19007669]
15. Neufeld G, Cohen T, Gengrinovitch S, Poltorak Z. Vascular endothelial growth factor (VEGF) and its receptors. FASEB J. 1999; 13:9–22. [PubMed: 9872925]
16. Prewitt RL, Chen IIH, Dowell RF. Development of microvascular rarefaction in the spontaneously hypertensive rat. Am. J. Physiol. 1982; 243:H243–H251. [PubMed: 7114235]
17. Rodrigues SF, Tran ED, Fortes ZB, Schmid-Schönbein GW. Matrix metalloproteinases cleave the beta2-adrenergic receptor in the spontaneously hypertensive rats. Am J Physiol. 2010; 299:H25–H35.
18. Struyker-Boudier HA, le Noble JL, Slaaf DW, Smits JF, Tangelder GJ. Microcirculatory changes in cremaster muscle during early spontaneous hypertension in the rat. J Hypertens Suppl. 1988; 6:S185–7. [PubMed: 3241198]
19. Tran ED, DeLano FA, Schmid-Schönbein GW. Enhanced matrix metalloproteinase activity in the spontaneously hypertensive rat: VEGFR-2 cleavage, endothelial apoptosis, and capillary rarefaction. J Vas Res. 2010; 47:423–431.
20. Tran ED, Schmid-Schönbein GW. An in-vivo analysis of capillary stasis and endothelial apoptosis in a model of hypertension. Microcirculation. 2007; 14:793–804. [PubMed: 17924279]
21. Vega F, Panizo A, Pardo-Mindan J, Diez J. Susceptibility to apoptosis measured by MYC, BCL-2, and BAX expression in arterioles and capillaries of adult spontaneously hypertensive rats. Am J Hypertens. 1999; 12:815–20. [PubMed: 10480475]

22. Vogt CJ, Schmid-Schönbein GW. Microvascular endothelial cell death and rarefaction in the glucocorticoid-induced hypertensive rat. Microcirculation. 2001; 8:129–39. [PubMed: 11379792]

23. Wang L, Dutta SK, Kojima T, Xu X, Khosravi-Far R, Ekker SC, Mukhopadhyay D. Neuropilin-1 modulates p53/caspases axis to promote endothelial cell survival. PLoS ONE. 2007; 2:e1161. [PubMed: 18000534]

24. Wang H, Olszewski B, Rosebury W, Wang D, Robertson A, Keiser JA. Impaired angiogenesis in SHR is associated with decreased KDR and MT1-MMP expression. Biochem Biophys Res Commun. 2004; 315:363–368. 26. Xiao YF, Wu DD, Liu SX, Chen X and Ren LF. (2007). Effect of arsenic trioxide on vascular endothelial cell proliferation and expression of vascular endothelial growth factor receptors Flt-1 and KDR in gastric cancer in nude mice. World J Gastroenterol 13:6498-6505. [PubMed: 14766216]

25. Xiao YF, Wu DD, Liu SX, Chen X, Ren LF. Effect of arsenic trioxide on vascular endothelial cell proliferation and expression of vascular endothelial growth factor receptors Flt-1 and KDR in gastric cancer in nude mice. World J Gastroenterol. 2007; 13:6498–6505. [PubMed: 18161919]

26. Zweifach BW, Kovalcheck S, DeLano FA, Chen P. Micropressure-flow relationship in a skeletal muscle of spontaneously hypertensive rats. Hypertension. 1981; 3:601–614. [PubMed: 7298115]

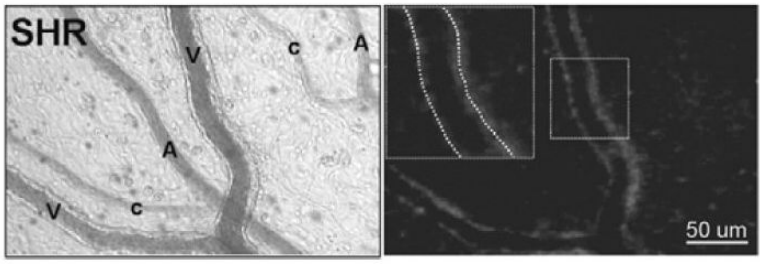

Figure 1.
Bright field (left) and fluorescent micrograph (right) with a MMP-7 substrate (see Methods) in the SHR mesentery microcirculation. The fluorescent activity is seen predominantly along venules (V) with lower levels along arterioles (A) and capillaries (C). Light intensity measurements were made by placement of a digital window over individual vessel segments (insert in right panel).

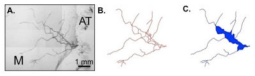

Figure 2.
Representative network montage (A), network tracing (B), and network area (C) from a SHR mesenteric microvascular network. The vascular area per network was defined as the area enclosed by connecting vessels (shaded blue region). “M” represents the mesenteric tissue region and “AT” represents bordering adipose tissue.

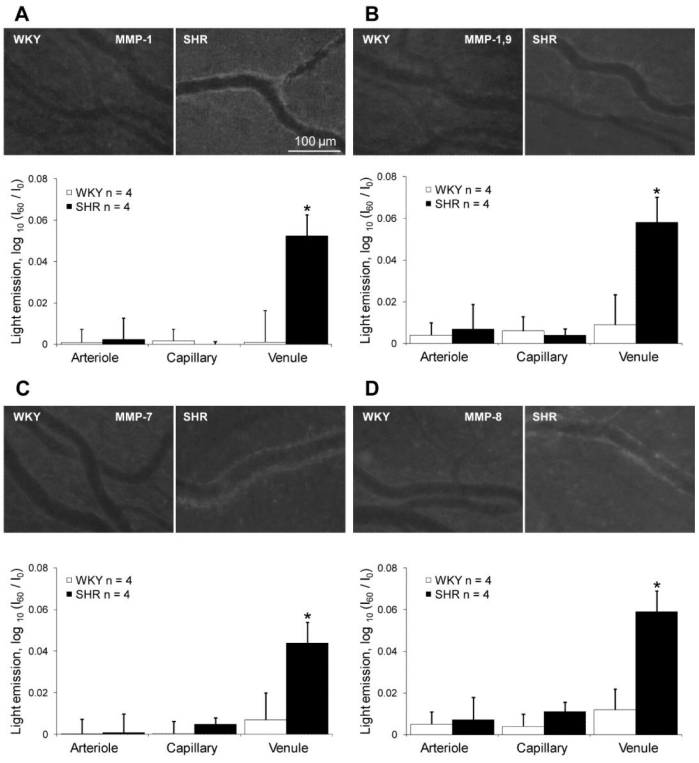

Figure 3.

Activity of MMPs in SHR microvascular endothelium. Top panels in A, B, C and D: Fluorescence micrographs generated by cleavage of intramolecularly-quenched substrate specific for MMP-1 (A), MMP-1/-9 (B), MMP-7 (C) and MMP-8 (D) in the mesenteric vessels of WKY and SHR. Bottom panels in A, B, C and D: I_{60} represents the average light intensity value along the vessel at 60 minutes after the substrate was loaded and I_0 represents the average light intensity value immediately after the substrate was loaded. Significantly increased MMP-1 -1/-9, -7, and -8 activities in the SHR were predominantly detected along venules, with lower activities along arterioles and capillaries. We did not detect enhanced activity of MMP-2 and -3 in the SHR (results not shown). n = number of animals, a minimum of 4 vessels per microvessel type.

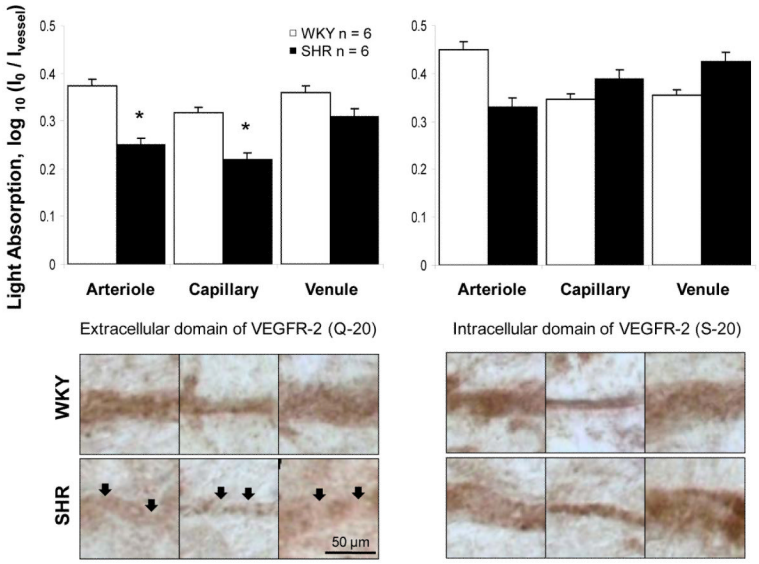

Figure 4.

Extracellular but not intracellular domain cleavage of VEGFR-2 in SHR vascular endothelium. Micrographs and light absorption measurements (bar graph) of immunohistochemical receptor density in the rat mesentery microvascular endothelium with separate antibodies against the extracellular (left panels) and intracellular (right panels) domain of the VEGFR-2 in WKY and SHR. I_{vessel} represents the average light intensity value along a vessel and I_0 represents the average light intensity value for a slide not containing a tissue. The SHR has a lower expression of extracellular domains of VEGFR-2 in mesenteric arterioles and capillaries, with a similar trend in venules (not significant) (arrows point to locations with lower VEGFR-2 extracellular label). n=6 rats for each group, 4 mesentery sectors per rat, and 8 measurements in each vessel type.

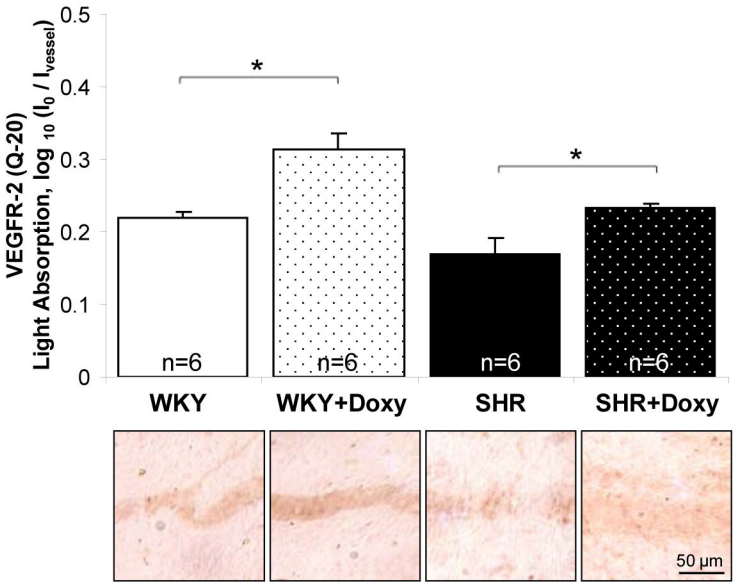

Figure 5.

Reversal of VEGFR-2 cleavage by chronic MMP inhibition. Immunohistochemical receptor density in the rat mesentery microvasculature was measured after labeling with antibody (Q-20) against the extracellular domain of the VEGFR-2 in the chronic doxycycline-treated WKY and SHR. I_{vessel} represents the average light intensity value along a vessel and I_0 represents the average light intensity value for a slide not containing a tissue. The doxycycline-treated WKY and SHR groups had significantly higher levels of the extracellular domain antibody labeling compared to their control groups, respectively.

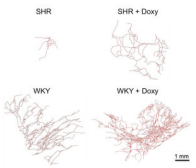

Figure 6.

Microvascular rarefaction is reversed by chronic MMP inhibition. Reconstructions of representative microvascular networks in the SHR and WKY rats before (left row) and after chronic MMP inhibition (+ Doxy group, right row). All microvessel segments were identified with PECAM labeling. Consistent with the rarefaction phenomenon typical SHR networks were smaller in comparison to typical WKY networks. Qualitatively, 71% (15/17) SHR networks had areas less than 0.5 mm^2 versus 25% (3/12) for the WKY networks. MMP inhibition served to increase the area of SHR networks; 18% (3/18) SHR + Doxy networks were less than 0.5 mm^2.

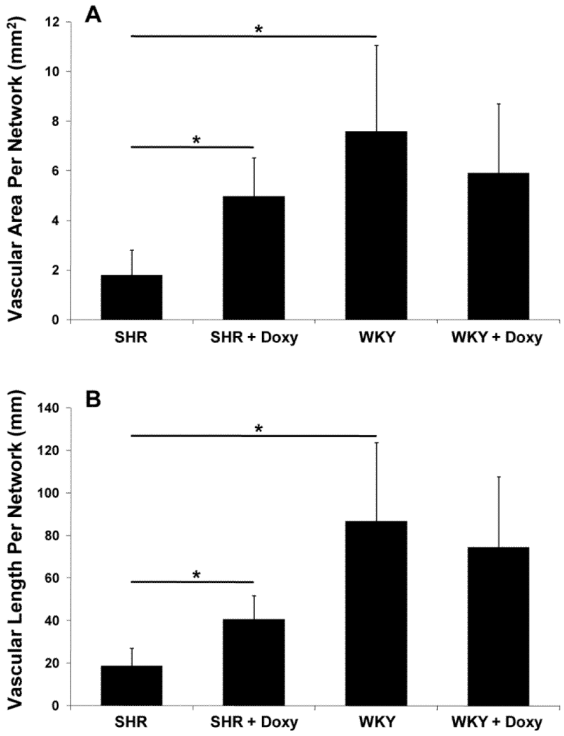

Figure 7.
(A) Vascularized area per network and (B) vascular length per network for SHR and WKY groups without and with chronic MMP inhibition with doxycycline (Doxy).

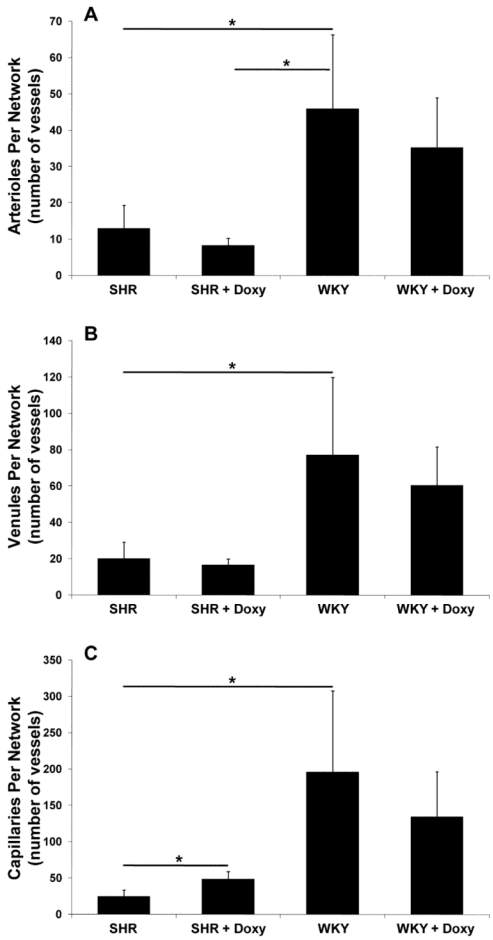

Figure 8.
Number of vessels per microvascular network in each vessel category for SHR and WKY groups without and with chronic MMP inhibition with doxycycline (Doxy). (A) Number of arterioles per network, (B) number of venules per network, and (C) number of capillaries per network.